Two Folded Conformers of Ubiquitin Revealed by High-Pressure NMR†

Ryo Kitahara, Hiroaki Yamada, and Kazuyuki Akasaka*

Department of Molecular Science, Graduate School of Science and Technology, Kobe University, 1-1 Rokkodai-cho, Nada-ku, Kobe 657-8501, Japan

Received May 7, 2001; Revised Manuscript Received July 12, 2001

ABSTRACT: High-pressure $^{15}N/^{1}H$ two-dimensional NMR spectroscopy has been utilized to study conformational fluctuation of a 76-residue protein ubiquitin at pH 4.5 at 20 °C. The on-line variable pressure cell technique is used in conjunction with a high-field NMR spectrometer operating at 750 MHz for ^{1}H in the pressure range between 30 and 3500 bar. Large, continuous and reversible pressure-induced ^{1}H and ^{15}N chemical shifts were observed for 68 backbone amide groups, including the 7.52 ppm ^{15}N shift of Val70 at 3500 bar, indicating a large-scale conformational change of ubiquitin with pressure. On the basis of the analysis of sigmoid-shaped pressure shifts, we conclude that ubiquitin exists as an equilibrium mixture of two major folded conformers mutually converting at a rate exceeding $\sim 10^4$ s^{-1} at 20 °C at 2000 bar. The second conformer exists at a population of ∼15% ($\Delta G^0 = 4.2$ kJ/mol) and is characterized with a significantly smaller partial molar volume ($\Delta V^0 = -24$ mL/mol) than that of the well-known basic native conformer. The analysis of ^{1}H and ^{15}N pressure shifts of individual amide groups indicates that the second conformer has a loosened core structure with weakened hydrogen bonds in the five-stranded β-sheet. Furthermore, hydrogen bonds of residues 67−72 belonging to β_5 are substantially weakened or partially broken, giving increased freedom of motion for the C-terminal segment. The latter is confirmed by the significant decrease in $^{15}N\{^{1}H\}$ nuclear Overhauser effect for residues beyond 70 at high pressure. Since the C-terminal carboxyl group constitutes the reactive site for producing a multi-ubiquitin structure, the finding of the second folded conformer with a substantially altered conformation and mobility in the C-terminal region will shed new light on the reaction mechanism of ubiquitin.

Proteins are generally believed to fold into a single conformation called "native structure". Refinement of native structure coordinates and study of associated dynamics are believed to give the golden way to the understanding of protein function (*1*−*3*). On the other hand, native structures of proteins are known to be only marginally stable in solution, meaning that they exist basically in equilibrium with other conformations involving an unfolded conformer and maybe other intermediate conformers. Furthermore, observation of heterogeneous hydrogen-exchange rates among individual amide groups of a protein suggests the presence of intermediate conformers (*4*−*6*), but the existence of such conformers has seldom been confirmed spectroscopically nor have their structures analyzed experimentally.

In the present report, we study conformational equilibrium in ubiquitin under closely physiological conditions, using the "on-line variable pressure cell" NMR[1] spectroscopy technique (*7*). Ubiquitin is a small (8565 Da) protein consisting of 76 amino acid residues with no disulfide bridges. It has a primary structure MQIFVKTLTG[10]KTITLEVEPS[20]-DTIENVKAKI[30]QDKEGIPPDQ[40]QRLIFAGKQL[50]-EDGRTLSDYN[60]IQKESTLHLV[70]LRLRGG, which is conserved in all animals so far examined (*8*). Ubiquitin is present in all eukaryotes and is considered to have crucial roles in many important cell functions (*8*), its primary role being to control ATP-dependent proteolysis of damaged proteins. In this process, ubiquitin forms a covalent bond with its carboxyl termini with a cysteine residue of enzyme E1 (ubiquitin activating protein), E2 (ubiquitin conjugating protein), or E3 (ubiquitin recognition protein) through a thioester bond (*8*). A multi-ubiquitin chain structure is further formed through isopeptide bonds between the carboxyl end of one ubiquitin molecule and a lysine amino group of another ubiquitin molecule. The multi-ubiquitin chain is known to function as a signal for the ATP-dependent proteolytic degradation of damaged proteins which takes place in proteasome (*8*, *9*).

The three-dimensional structure of ubiquitin has been studied in crystal by X-ray diffraction (*10*) and in solution by NMR (*3*, *11*, *12*), both of which report essentially the same conformer. It forms a core consisting of a five-stranded β-sheet (two parallel inner strands, 1−7 and 64−72, and three other strands, 10−17, 40−45, and 48−50), an α-helix (residues 23−34), a short 3_{10}-helix (residues 56−59), and loops. Because, in the multi-ubiquitin chain structure, ubiquitin forms an intermolecular covalent bond through the

† This work was supported by a Grant-in-Aid for Scientific Research from the Ministry of Education, Culture, Sports, Science, and Technology of Japan (12480201).

* To whom correspondence should be addressed. Present address: Cellular Signaling Laboratory, RIKEN Harima Institute, 1-1-1 Kouto, Mikazuki-cho, Sayo-gun, Hyogo 679-5148, Japan. E-mail: akasaka8@spring8.or.jp. Phone: +81-791-58-0802- (voice) -0-3359. Fax: +81-791-58-2835.

[1] Abbreviations: NMR, nuclear magnetic resonance; HSQC, heteronuclear single-quantum correlation; NOE, nuclear Overhauser effect; DSS, 2,2-dimethyl-2-silapentane-5-sulfonate.

10.1021/bi010922u CCC: $20.00
Published on Web 10/16/2001

C-terminal carboxyl group, detailed information on the conformation and the dynamics of the C-terminal segment is crucially important for understanding the molecular mechanisms of ubiquitin function. So far, X-ray crystallography has shown enhanced *B*-factors for the C-terminal four residues 73−76 (*10*), while ^{15}N spin relaxation studies have revealed the presence of rapid internal motions of subnanosecond range for the polypeptide backbone of the same part (*1*, *2*). These observations indicate that the C-terminal four residues are free from the core part. However, measurements of hydrogen-exchange rates of individual amide protons have shown that the rate is extremely high for six residues, 71−76, rather than 73−76, suggesting an alternative possibility that the entire segment 71−76 may be free from the core part (*13*). These discrepancies may arise because of different time ranges of motion detected by different methods and because of the environmental difference, i.e., solid against solution.

We have recently developed a new method for detecting protein conformational fluctuation using high-pressure NMR (*14*−*18*). The method is sensitive to conformational fluctuation in a much wider time range than that of the spin relaxation, namely, from subnanosecond to at least about millisecond using chemical shift (*15*) or even in a much slower time range (greater that millisecond) using line shape (*14*) or signal intensity (*16*−*18*). Furthermore, the method detects conformational fluctuation in a much wider conformational space than hitherto explored by enhancing the population of rare conformers under pressure that are usually neglected spectroscopically (*16*−*18*). Thus fluctuation to a hitherto unknown conformer is likely to be detected by this method. In the present report, first a comparative experiment of ^{15}N{^{1}H} heteronuclear spin relaxation (NOE) at 30 and 3000 bar is reported. Then, pressure-induced ^{15}N and ^{1}H chemical shifts are recorded for individual amide groups on ^{15}N uniformly labeled human ubiquitin. In this experiment, the explored pressure range is extended up to 3500 bar, compared to 2000 bar in most of our previous experiments, to record the pressure-shift profile as completely as possible. The results are used to probe site-specific conformational fluctuations in a much wider time range and in a much wider conformational space than hitherto explored in ubiquitin.

MATERIALS AND METHODS

Sample Preparation. Uniformly ^{15}N-labeled ubiquitin was purchased from VLI Co. Samples for high-pressure NMR chemical shift measurements were prepared by dissolving ^{15}N-labeled ubiquitin in 30 mM acetate-d_3 buffer (pH 4.5 at 25 °C) containing 5% ^2H_2O at a concentration of 2.0 mM. The same buffer was used for measurements of heteronuclear ^{15}N{^{1}H} NOE at a protein concentration of 3.5 mM.

High-Pressure NMR Measurements. High-resolution, high-pressure NMR experiments were performed on a Bruker DMX-750 spectrometer combined with the on-line high-pressure NMR cell technique (*7*). The pressure-resistive sample cell consists of a long capillary tube, the end part of which has a body of an inner diameter less than 1 mm and an outer diameter of ∼3 mm, which holds the sample solution of ca. ∼20 μL. The sample solution is separated from the pressure mediator (kerosene) by Teflon pistons in a separator cylinder made of BeCu, and the pressure of the sample solution is controlled with a remotely located hand pump.

For measurements of chemical shifts, a highly pressure-resistive sample cell was prepared that endures pressure up to ∼4000 bar. ^{15}N/^{1}H HSQC spectra were measured with a standard HSQC sequence (*19*) combined with a WATERGATE technique with a 3-9-19 pulsed field gradient (*20*) at a proton frequency of 750.13 MHz and an ^{15}N frequency of 76.01 MHz. The ^{15}N dimension was acquired with 256 increments, and for the proton dimension 2048 complex points were collected with an offset at the residual water signal. The data were processed with the XWIN-NMR package (Bruker) running on a Silicon Graphics O2 workstation. Spectra were zero-filled to give a final matrix of 4096 × 512 real data points and apodized with a 90° shifted sine-bell window function in both dimensions. At all pressures, ^{1}H chemical shifts were referenced to the methyl signal of 2,2-dimethyl-2-silapentane-5-sulfonate (DSS), and ^{15}N chemical shifts were indirectly referenced to DSS (0 ppm for ^{1}H) and dioxane (3.75 ppm for ^{1}H). The inertness of the DSS chemical shift to pressure is partly assured by the invariance of the chemical shift difference between DSS and dioxane against pressure. The pH change of an acetate buffer solution at 3500 bar is expected to be about −0.6 pH unit from the known ionization volume of acetate (*21*). Heteronuclear ^{15}N-{^{1}H} nuclear Overhauser effect (NOE) was measured at 30 and 3000 bar at 20 °C and pH 4.7 in a different sample cell that can endure pressure up to 3000 bar. Spectra were recorded with and without presaturation of the amide proton signals for 3.0 s with a relaxation delay of 1.0 s (*22*), and each data set was acquired with 1200 (^{1}H) × 256 (^{15}N) complex data points and 100 scans. NOE values were obtained as ratios of peak heights with and without proton saturation.

Thermodynamic Analysis. For the case that the two conformers are in rapid exchange in the NMR time scale, the observed chemical shift δ is related to the equilibrium constant K_{obs} by the relation:

$$K_{obs} = \frac{\delta_{N1} - \delta}{\delta - \delta_{N2}} \qquad (1)$$

where δ_{N1} and δ_{N2} are the intrinsic chemical shifts of the two conformers, N_1 and N_2, respectively, and δ is the observed chemical shift at a given pressure. In eq 1, caution must be taken to include the fact that δ_{N1} and δ_{N2} themselves vary with pressure owing to a general compaction of a protein molecule under pressure (*14*, *15*). Fortunately, the variation of chemical shift due to this effect is almost linear with pressure (*23*, *24*), typical slopes of which are 1.5×10^{-4} ppm/bar for ^{15}N and 6.0×10^{-5} ppm/bar for ^{1}H as average values in the β-sheet region of a stable globular protein BPTI (*15*).

On the other hand, the Gibbs energy difference between any two conformers is expressed as a function of pressure p by eq 2 under the assumption of no compressibility change with pressure:

$$\Delta G^p = -RT \ln K_{obs} = \Delta G^0 + \Delta V^0 (p - p_0) \qquad (2)$$

Here R is the gas constant, T is the absolute temperature, K_{obs} is the observed equilibrium constant, and ΔG^p and ΔG^0 are the Gibbs free energy differences at pressure p and p_0 (=1 bar), respectively. ΔV^0 is the partial molar volume

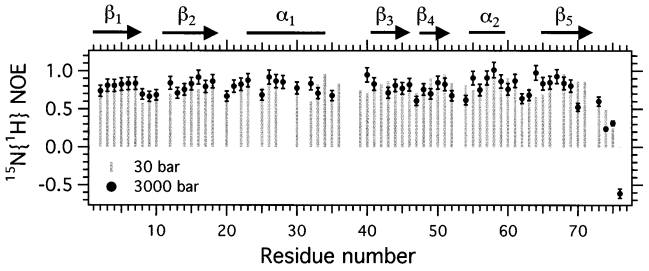

FIGURE 1: Heteronuclear $^{15}N\{^1H\}$ steady-state NOEs of ubiquitin at 30 bar (gray bars) and at 3000 bar (filled circles) at 20 °C. Black bars show uncertainties (±10%) of the experimental values estimated from two data sets. To avoid complication, the uncertainties are put only on the data at 3000 bar. Locations of the secondary structural elements are shown for α-helices (lines) and β-strands (arrows) at the top of the figure. The NOE data of residues 13, 21, 28, 31, 67, and 72 at 30 bar and residues 31, 34, 39, 42, 71, and 72 at 3000 bar are not available because of the overlap of cross-peaks.

difference between the two conformers at pressure p_0 (=1 bar). By combining eqs 1 and 2, the chemical shift is expressed as a function of pressure by

$$\delta = \frac{\delta_{N1} + \delta_{N2} \exp\left\{-\dfrac{\Delta G^0 + \Delta V^0(p - p_0)}{RT}\right\}}{1 + \exp\left\{-\dfrac{\Delta G^0 + \Delta V^0(p_1 - p_0)}{RT}\right\}} \quad (3)$$

Chemical shift values experimentally determined at various pressures are fitted to eq 3 by four parameters, δ_{N1}, δ_{N2}, ΔG^0, and ΔV^0.

Analysis of Exchange Line Broadening. For a fast two-site exchange, the line width at half-intensity $\Delta\nu_{1/2}$ (Hz) of a homogeneously broadened resonance is given by

$$\pi\Delta\nu_{1/2} = \frac{P_A}{T_2^A} + \frac{P_B}{T_2^B} + \frac{P_A P_B(\delta\omega)^2}{1/\tau_A + 1/\tau_B} \quad (4)$$

where T_2^A and T_2^B are intrinsic transverse relaxation times of site A and site B, respectively, P_A and P_B are the populations of A and B, $\delta\omega$ (rad·s^1) is the chemical shift difference in angular frequency between the two sites, and $1/\tau_A$ and $1/\tau_B$ are the exchange rates from site A to site B and from site B to site A, respectively (*25*). Lower limits of the exchange rates are given from eq 4 for the case that the intrinsic transverse relaxation times T_2^A and T_2^B are assumed to be infinite.

RESULTS

^{15}N spin relaxation is a well-established method for probing backbone dynamics of proteins (*26*, *27*) and was previously used to analyze the dynamics of ubiquitin (*1*, *2*). First, we have applied the same technique to probe nanosecond to picosecond dynamics of ubiquitin by measuring $^{15}N\{^1H\}$ nuclear Overhauser effect (NOE). The residue-specific variation of NOE at 30 bar (Figure 1) almost coincided with that reported by Lienin et al. (*1*), measured at 1 bar in a normal sample tube at 600 MHz, namely, the NOE values are slightly smaller in most loop regions than in the regions forming secondary structures and that NOE values for residues 73−76 are particularly small, indicating rapid internal motions of the main chain of these residues.

We have extended measurements of heteronuclear $^{15}N\{^1H\}$ NOE values at 3000 bar at 20 °C (Figure 1). By increasing pressure to 3000 bar, changes in NOE values are almost negligible or very small for most residues, and a substantial decrease in NOE relative to that at 30 bar was

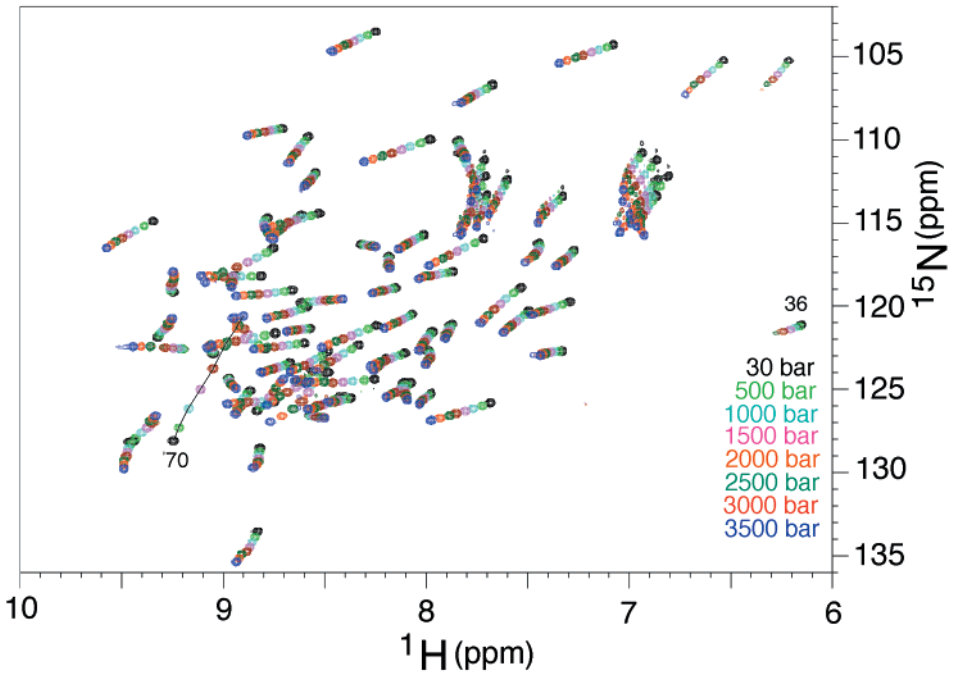

FIGURE 2: Superposition of $^{15}N/^1H$ HSQC spectra of ^{15}N uniformly labeled ubiquitin recorded at various pressures from 30 to 3500 bar at 20 °C (black, 30 bar; light green, 500 bar; blue, 1000 bar; pink, 1500 bar; brown, 2000 bar; green, 2500 bar; red, 3000 bar; and purple, 3500 bar). The protein is dissolved to a concentration of 2.0 mM in 30 mM acetate buffer (95% ^1H_2O/5% ^2H_2O, pH 4.5). The cross-peaks of Val70 are traced with a line for easy recognition.

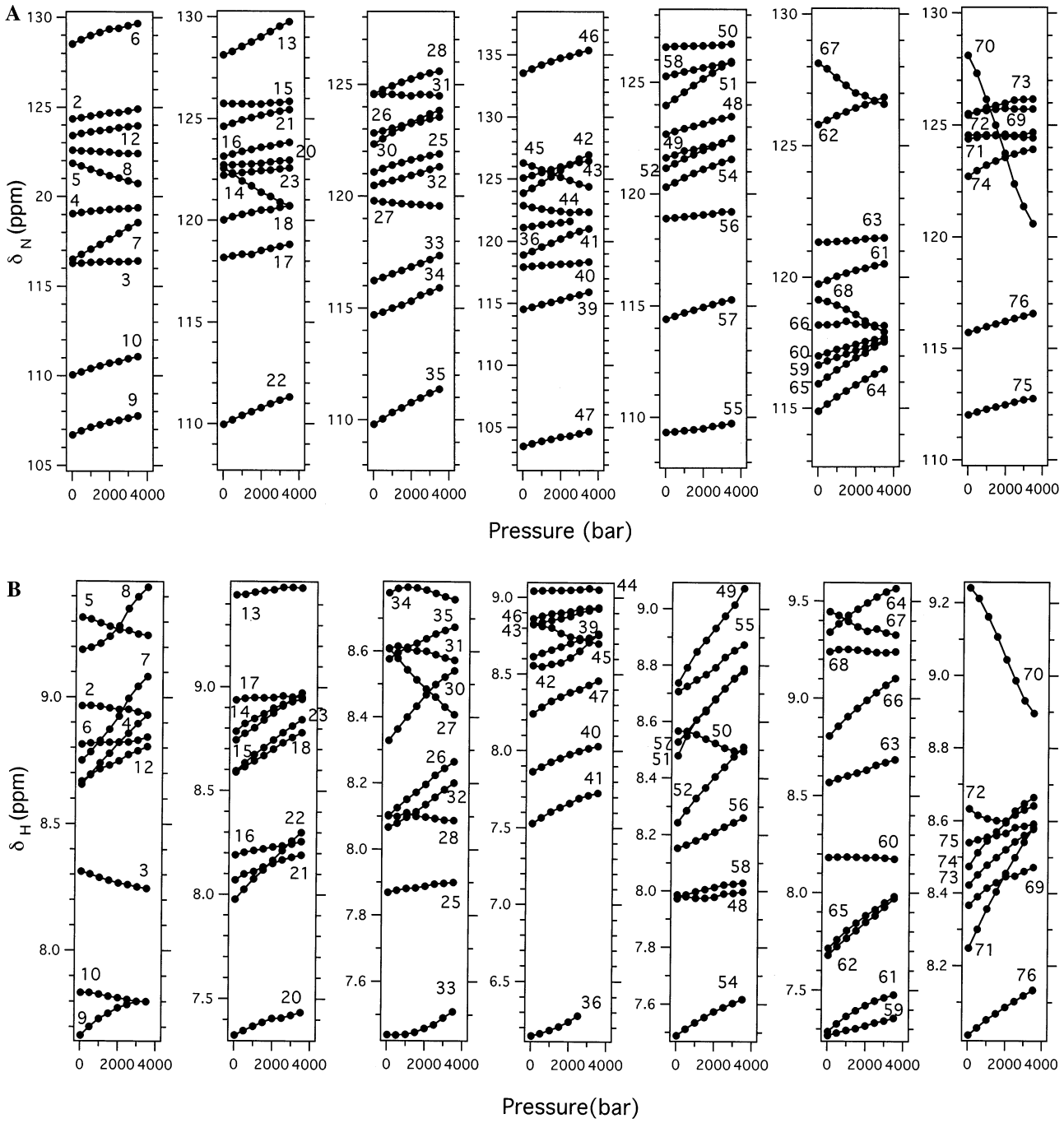

FIGURE 3: Plots of ^{15}N (panel A) and ^{1}H (panel B) chemical shifts of individual main chain amide groups of ubiquitin as a function of pressure between 30 and 3500 bar at 20 °C. Numbers in the figure denote residue numbers.

observed only for residues 70, 72, and 74 in the C-terminal segment. These observations tell qualitatively that subnanosecond motions are increased at high pressure specifically in the C-terminal segment. The result suggests that at high pressure the conformation of ubiquitin is different from that at 1 bar in that the C-terminal segment is substantially more free.

Pressure-induced chemical shift changes have newly emerged as sensitive means of detecting site-specific fluctuation of protein conformation (*15*). Figure 2 shows a superposition of $^{15}N/^{1}H$ two-dimensional HSQC spectra of ^{15}N uniformly labeled ubiquitin recorded at 500 bar intervals between 30 and 3500 bar at 20 °C. $^{15}N/^{1}H$ chemical shifts of individual cross-peaks at 30 bar are identical with those at 1 bar, which have been assigned to individual amino acid residues by Wang et al. (*28*). All of the cross-peaks showed reversible chemical shift changes, thereby allowing extension of the assignments established at 1 bar to any pressure. Their signal intensities do not change with pressure except for Ile36, whose intensity decreases with pressure. While the substantial shift changes indicate a substantial conformational change at high pressure, the fact that the signals remain well dispersed up to 3500 bar also indicates that the protein remains folded throughout the pressure change studied at 20 °C. Thus the phenomenon is completely different from the pressure-assisted cold denaturation of ubiquitin found by Nash and Jonas at pH 3, −16 °C, and 2250 bar (*29*) and the pressure-induced denaturation of ubiquitin found by Schick

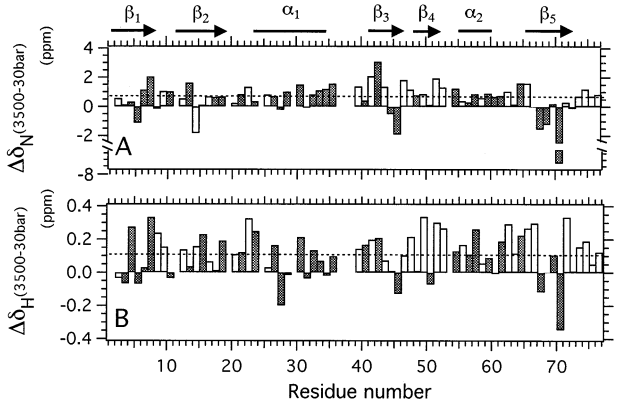

FIGURE 4: Pressure-induced chemical shifts ($\Delta\delta = \delta_{3500bar} - \delta_{30bar}$) of amide ^{15}N (panel A) and ^{1}H (panel B) plotted against the amino acid sequence of ubiquitin. The shaded columns are for the amide groups that are internally hydrogen bonded with carbonyls, and the open columns are for the rest of the amide groups. Hydrogen-bonding partners are determined by a program MOLMOL with constraints of the hydrogen bond length (H^N---O^C distance < 2.4 Å) and the angle (N−H---O angle > 145°) in ten NMR structures (*3*). The average values of ^{15}N (0.67 ppm) and ^{1}H (0.11 ppm) pressure shifts are shown by dotted lines. Pressure effects are classified according to the shift deviations from the averages.

at pH 2, 25 °C, and 3000 bar (*30*). Only the cross-peak of Ile36 preferentially broadens and disappears at 3000 bar, suggesting a selective conformational fluctuation at its backbone with increasing pressure. This phenomenon is likely to originate from the deformation or hydration of the cavity formed partly by the side chain of Ile36 (cf. Figure 5A). Otherwise, the preferential broadening of the Ile36 cross-peak may be correlated to the cis−trans isomerization of two trans prolines (Pro37 and Pro38) at high pressure.

The ^{15}N and ^{1}H chemical shifts of all of the 68 cross-peaks of the main chain amide groups are plotted as functions of pressure in Figure 3 (panel A, ^{15}N, and panel B, ^{1}H). A notable feature in these figures is that exceptionally large pressure-induced chemical shift changes are observed for many residues, especially that several ^{15}N signals (residues 5, 14, 45, 67, 68, and 70) exhibit large high-field shifts (>1 ppm at 3500 bar) with increasing pressure. Another notable feature is that many of the shifts are distinctly *nonlinear* with pressure, some of which clearly show *sigmoidal* character, for example, residues 70, 67, and 68 in Figure 3A and residues 70, 7, 8, 49, 50, 68, and 69 in Figure 3B.

Figure 4 visualizes changes in pressure-induced ^{15}N and ^{1}H chemical shifts at 3500 bar as histograms for individual backbone amide groups (panel A, ^{15}N, and panel B, ^{1}H). The shaded columns are for the amide groups that are internally hydrogen bonded with carbonyl groups, while the open columns are for the rest of the amide groups that are presumably hydrogen bonded with solvent water. The average changes in ^{15}N chemical shifts excluding Val70 are 0.67 ± 0.90 ppm (average ± RMS) at 3500 bar, while the average changes in ^{1}H chemical shifts are 0.11 ± 0.14 ppm at 3500 bar (shown by the dotted lines in the figure). Residues showing unusually large shifts do not exactly match between ^{15}N and ^{1}H. This is not surprising because of the difference in shift mechanisms for the two nuclei (*15*, *23*). For the amide protons, the ^{1}H shift is correlated with the H−O hydrogen bond distance (*23*, *31*), while the ^{15}N shift is more sensitive to torsion angles (*15*, *32*).

DISCUSSION

Information Obtained from Heteronuclear $^{15}N\{^{1}H\}$ NOE Measurements. Spin relaxation measurements including NOE give dynamics information in the picosecond to nanosecond time range (*26*, *27*). Changes in heteronuclear $^{15}N\{^{1}H\}$ NOE measurements in ubiquitin at 20 °C by increasing pressure to 3000 bar are rather small (Figure 1). However, substantial decreases in NOE are clearly observed for some residues in the C-terminal segment at 3000 bar. A gradual decrease in the NOE values beyond residue 67 at 3000 bar shows that the restriction of backbone dynamics between residues 67 and 72 at 30 bar is relieved. In particular, the NOE values for residues 70, 74, and 76 are decreased to 0.52, 0.23, and −0.61, respectively, at 3000 bar. Such small NOE values indicate that these residues are quite freely moving at high pressure, showing the possibility that a substantial conformational change takes place in the C-terminal segment, residues 67−76, such that a large part of the C-terminal segment becomes free at high pressure. Overall, change in picosecond to nanosecond dynamics with pressure is relatively small, but the suggestion is obtained for a conformational change in the C-terminal region.

Evidence for the Second Folded Conformer. Conformational fluctuation of a protein in a much wider time range (up to about millisecond) is obtainable from chemical shift measurements as a function of pressure (*15*). Almost all residues show significant and reversible ^{1}H and ^{15}N chemical shift changes with pressure (Figure 3), although clear NOE changes were detected only for residues beyond 70 (Figure 1). Interestingly, many of these chemical shifts are nonlinear with pressure, suggesting that a conformational change other than a general compaction of the protein molecule is taking place (*33*). Furthermore, several of them show clearly sigmoidal character superimposed on the linear shifts. Residues showing the sigmoidal character are found at different parts of the protein molecule, namely, residues 7 and 8 (β_1), 49 and 50 (β_4), and 68, 69, and 70 (β_5) for ^{1}H and residues 67, 68, and 70 (β_5) for ^{15}N between 30 and 3500 bar. Moreover, the sigmoidal chemical shift changes for different residues occur nearly in the same pressure range centering around 2000 bar. These results indicate that ubiquitin undergoes a conformational change with pressure simultaneously at different sites of the protein, suggesting a cooperative conformational transition of the entire protein molecule.

In Figure 3, the sigmodal-shaped chemical shift changes are totally missing or not clearly observed for many residues except for those mentioned above. This is understood as a result of superposition of a linear chemical shift change due to the general compaction of the protein molecule onto a sigmoidal-shaped shift due to a conformational transition. When the chemical shift change due to the transition is small relative to the chemical shift change due to the compaction, the sigmoidal character of the shift would be hardly recognizable. This is likely to be the case for many residues for which the sigmoidal character of the shift is not clear. Such a situation is reasonably expected if the transition involves a major change of the structure in selected regions of the protein molecule and a minor change for the rest of the protein molecule, as previously encountered in other proteins (*17*, *18*). Overall, the chemical shift variations in

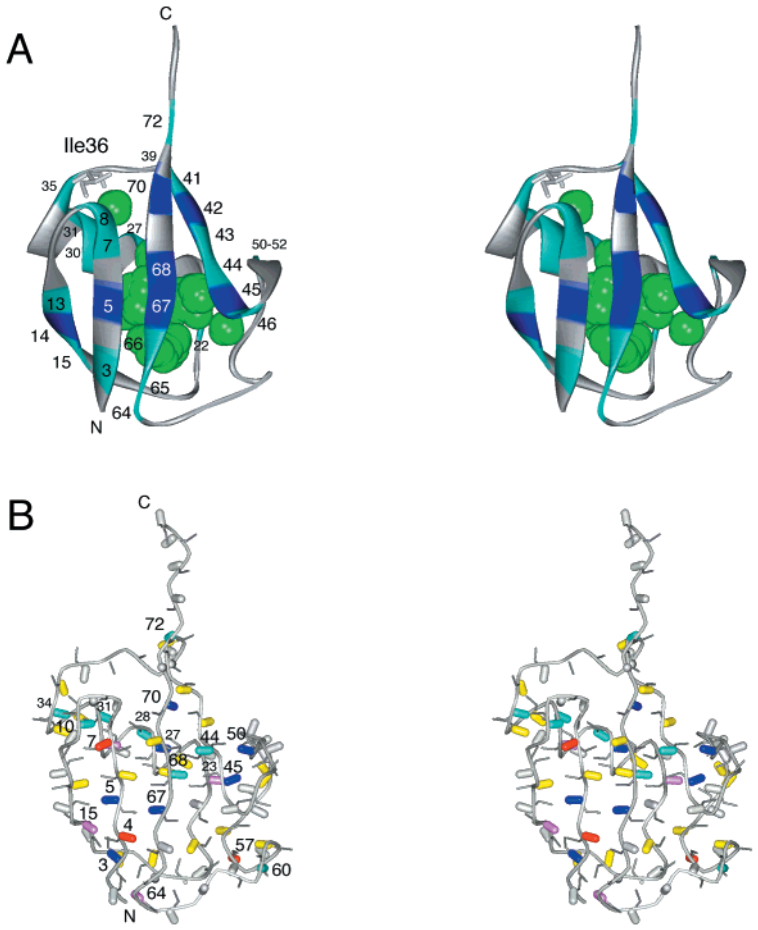

FIGURE 5: (A) Location of residues showing anomalous amide ^{15}N pressure shifts on the three-dimensional X-ray structure of ubiquitin (PDB: 1UBQ) (*10*). The residues showing anomalous amide nitrogen shifts are marked by colors according to their deviation ($\Delta\delta$) from the average pressure shift (+0.67 ppm at 3.5 kbar): $\Delta\delta > +1.50$ ppm or $\Delta\delta < -1.50$ ppm (purple), $+1.50$ ppm $> \Delta\delta > +0.60$ ppm or -0.60 ppm $> \Delta\delta > -1.50$ ppm (blue) (cf. Figure 4A). Cavities calculated with the program GRASP (*34*) with a probe radius of 1.0 Å are represented by green spheres. Ile36 whose cross-peak preferentially broadens and disappears at 3000 bar is drawn in stick format. (B) Location of residues showing anomalous amide ^{1}H pressure shifts on a representative NMR structure of ubiquitin (PDB: 1D3Z) (*3*). The internally hydrogen-bonded amide groups that show anomalous ^{1}H pressure shifts are marked by colors according to their deviation ($\Delta\delta$) from the average pressure shift (+0.11 ppm at 3.5 kbar): $\Delta\delta > +0.15$ ppm (red), $+0.10 < \Delta\delta < +0.15$ ppm (pink), $-0.10 < \Delta\delta < +0.10$ ppm (yellow), $-0.15 < \Delta\delta < -0.10$ ppm (blue), and $\Delta\delta < -0.15$ ppm (purple) (cf. Figure 4B). The NH and CO groups are represented in thick and thin stick format, respectively. These diagrams are drawn by WebLab ViewerLite 3.2.

Figure 3 appear to be most reasonably interpreted as resulting from a cooperative-type reversible conformational transition between two major conformers of ubiquitin, namely, the well-known folded conformer ("native" structure, N_1) at 1 bar (*3*, *10*) and another conformer, N_2, stabilized at high pressure. Since the chemical shift dispersion remains large for most signals even at 3500 bar, the transition must occur more or less within the folded manifold of the protein. The existence of an alternative fold of ubiquitin (N_2), differing from the well-established basic folded conformer N_1 determined by X-ray diffraction in the crystal (*10*) and by NMR in solution (*3*), has not been reported previously.

Structure of the Second Folded Conformer Inferred from ^{1}H and ^{15}N Shifts. Clear sigmoidal-shaped shifts are manifested by residues 7, 8, 49, 50, 68, 69, and 70 for ^{1}H and residues 67, 68, and 70 for ^{15}N. In particular, residue 42 (the hydrogen-bonding pair of residue 70) exhibits an anomalous ^{15}N shift deviation of more than +1.50 ppm (low-field shift) from the average pressure shift (+0.67 ppm) at 3500 bar, while the residues 5, 14, 45, 67, 68, and 70 show anomalous ^{15}N shift deviation of less than −1.50 ppm (high-field shift) from the average pressure shift (+0.67 ppm) at 3500 bar. The locations of amino acid residues showing anomalous ^{15}N pressure shifts are marked by colors on the three-dimensional X-ray structure of ubiquitin (*10*) (Figure 5A) according to the magnitude of the shift deviation ($\Delta\delta$) from the average shift: $\Delta\delta > +1.5$ ppm or $\Delta\delta < -1.5$ ppm (purple), $-1.5 < \Delta\delta < -0.6$ ppm or $+0.6 < \Delta\delta < +1.5$ ppm (blue). The locations of internal cavities calculated using the program GRASP (*34*) are also shown in green.

For those amide groups that are internally hydrogen bonded with carbonyls, the amide ^{1}H chemical shift is closely related to the hydrogen bond distance (*23*, *31*). In Figure 4B (^{1}H), we have classified the NH groups hydrogen bonded with carbonyls into five classes according to the magnitude of the shift deviation ($\Delta\delta$) from the average shift (0.11 ppm/3.5 kbar) and marked them with colors on the three-dimensional NMR structure of ubiquitin (*3*) (Figure 5B): $\Delta\delta > +0.15$ ppm (red), $+0.10 < \Delta\delta < +0.15$ ppm (pink), $-0.10 < \Delta\delta < +0.10$ ppm (yellow), $-0.15 < \Delta\delta < -0.10$ ppm (blue), and $\Delta\delta < -0.15$ ppm (purple).

The ^{1}H high-field shift (purple and blue) and the low-field shift (red and pink) beyond the average are considered to be correlated with the elongation and the shortening of

the NH—O═C hydrogen bond distance, respectively (*23*), while the anomalous ^{15}N shifts (purple) are likely to represent changes in backbone torsion angles (*15*). It is clear from Figure 5A that the structural difference between N_1 and N_2 involves four β-strands, in particular, their central regions holding the clustered cavities. The backbone torsion angles (ψ and ϕ) and hydrogen bond geometry must be significantly altered in these regions. Residues Val70, His68, and Leu67 show particularly large ^{15}N pressure shifts toward high field (7.52, 1.22, and 1.54 ppm, respectively, at 3500 bar). An empirical relation $\Delta\delta_{15N}(\text{ppm}) = -0.2325\psi$ (degree) has been presented between the ^{15}N shift and torsion angle ψ for the β-sheet region of BPTI (*15*). If we straightforwardly apply this empirical equation to the ^{15}N chemical shifts of 7.52, 1.22, and 1.54 ppm for Val70, His68, and Leu67 of ubiquitin, respectively, we predict changes in ψ angles of 32, 5, and 7 degrees, respectively, which would result in a total alteration of the native orientation (N_1) of the C-terminal segment. The result indicates that the backbone conformation in N_2 is substantially different in the segment beginning at residue 67 and beyond.

In accordance with this, the large high-field shifts of Ile44, Leu67, His68, and Val70 amide protons support the view that the hydrogen bond interactions with the β-strands of both sides are substantially weakened; for example, the elongation of the NH—O═C hydrogen bond distances between Phe45 NH and Lys48 CO and between Leu50 NH and Leu43 CO are suggested (Figure 5B). In addition, the chemical shift values for amide protons of the C-terminal segment, residues Leu71, Arg72, Leu73, Arg74, and Gly75 (except for that of the C-terminal residue Gly76 showing a high-field shift due probably to the effect of the charged carboxyl end), tend to cluster in a small chemical shift region between 8.5 and 8.7 ppm with increasing pressure (Figure 3B). The random coil ^{1}H chemical shifts for amide protons of Gly, Leu, and Arg are 8.3−8.5 ppm at 1 bar and 35 °C (*35*). When considering the fact that amide protons in an exposed or unfolded polypeptide chain shift toward low field with increasing pressure by ~0.1 ppm/2000 bar (*23*, *36*) and additionally by lowering temperature, the chemical shifts of residues 71−75 at 3500 bar at 20 °C (8.5−8.7 ppm) nearly coincide with those expected for an exposed or unfolded polypeptide chain, strongly suggesting that the entire C-terminal segment, residues 70−76, is close to "unfolded" in N_2. This means that the internal hydrogen bonds formed by residues 67−72 of β_5 with β_1 and β_3 strands are considerably weakened or broken at least partially.

Nitrogen shifts (Figure 5A) also indicate that a substantial structural change takes place in the central part of the molecule consisting of four β-strands. The region is close to the cluster of cavities, and the conformational change is apparently related to the deformation or hydration of these cavities. Correspondingly, we find a number of anomalous high-field shifts (purple) of amide ^{1}H signals in the central part of the β-sheet (Figure 5B). A high-field shift of an amide ^{1}H signal is generally correlated with the elongation of the hydrogen bond (*23*), meaning that the four-stranded β-sheet expands in the central part in N_2. All of the information above points to a notion that a concerted conformational change takes place in the central core region and the C-terminal segment beyond residue 67 becomes substantially freed in the second conformer, N_2.

Table 1: Limiting Amide ^{15}N and ^{1}H Chemical Shifts (δ_{N1}, δ_{N2}) of Val70, Gibbs Energy Change (ΔG^0), and Partial Molar Volume Change (ΔV^0) Associated with the Conformational Transition from the Basic Folded Conformation (N_1) to the Second Folded Conformation of Ubiquitin (N_2) at 20 °C at 1 bar

nucleus	δ_{N1} (ppm)	δ_{N2} (ppm)	ΔG^0 (kJ/mol)	ΔV^0 (mL/mol)
^{15}N	129.97	118.80	3.9 ± 0.4	-23 ± 2
^{1}H	9.30	8.82	4.6 ± 0.3	-25 ± 2

Dynamics of Fluctuation between the Two Conformers. The observed single resonance for Val70 should be the average resonance for two conformational sites of the peptide bond, indicating that the exchange rate between the two native conformers is much faster than their chemical shift separation ($\delta\omega = 2\pi \times 360$ rad·s^{-1}) (see Table 1). For the case that two conformers are present in equal populations ($P_A = P_B$ and $1/\tau_A = 1/\tau_B$, see Materials and Methods), the lower limit of the exchange rate calculated from eq 4 with the observed line width of the averaged peak (22 Hz) is ~10^4 s^{-1} at 20 °C and 2000 bar (see Materials and Methods).

Recently, we have encountered another case of the conformational equilibrium between two folded conformers in folate-bound dihydrofolate reductase from *Escherichia coli* (159 residues) (*17*), in which case the two native conformers are in slow exchange (<20 s^{-1}) with respect to chemical shift differences, thereby showing two distinct signals as opposed to the present case. In both proteins, a conformational change involving the entire protein molecule is involved. The rate of exchange depends apparently on the size of the protein beside other factors. However, the rate is definitely slow, compared to the subnanosecond to nanosecond range monitored by spin relaxation since our NOE measurements (Figure 1) showed no hint of corresponding motions involving the central portion of the β-sheet.

Thermodynamic Properties of the Second Folded Conformer. Pressure-induced spectral changes observed in the present experiment are totally reversible with pressure, meaning that the two folded conformers, N_1 and N_2, are in thermodynamic equilibrium at all pressures studied. Thus, the thermodynamic stability of N_2 relative to that of N_1 can be evaluated on the basis of eqs 1−3. Pressure-induced changes in both ^{15}N and ^{1}H chemical shifts of Val70 are used to calculate the Gibbs free energy difference (ΔG^0) and the partial molar volume difference (ΔV^0) between N_1 and N_2 by fitting eq 3 (see Materials and Methods) to the ^{1}H and ^{15}N shift data for residue 70 (Figure 6). ΔG^0_{N2-N1} and ΔV^0_{N2-N1} values are determined as averages of two calculations for ^{15}N and ^{1}H chemical shifts to be 4.2 ± 0.4 kJ/mol and -24 ± 2 mL/mol, respectively, at 1 bar and 20 °C. The ΔG^0 value predicts a population of N_2 of 15 ± 2% at 1 bar and 20 °C. The negative volume change (−24 mL/mol) for the transition from N_1 to N_2 is likely to be caused by a partial loss or a rearrangement of the cluster of cavities in the central part of the β-sheet probably accompanied by entry of water molecules (Figure 5A). This would be accompanied by conformational changes in the backbone structures in the central part of the β-sheet and in the C-terminal β-strand (residues 67−76).

Functional Significance of the Second Folded Conformer. Our finding indicates that ubiquitin exists, under physiological conditions, as a dynamic mixture of two major conformers, namely, the well-known conformer N_1 (~85% at 20 °C

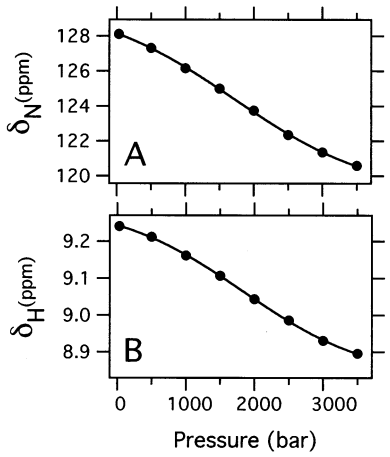

FIGURE 6: Pressure dependence of ^{15}N (panel A) and ^{1}H (panel B) chemical shifts of Val70 at 20 °C. Solid lines show the best-fit curves of eq 3 with the four parameters (δ_{N1}, δ_{N2}, ΔG^0, and ΔV^0) listed in Table 1.

at 1 bar) whose backbone is held rigid up to residue 72 and the second folded conformer N_2 (~15% at 20 °C at 1 bar). The structures of the two conformers differ substantially, N_2 having a longer free C-terminal segment from residue 70 to residue 76 with the hydrogen-bonding network for residues 70−72 likely to be broken and a partially hydrated core with a substantially expanded β-sheet. The C-terminal carboxyl being the reactive site, N_2 with a long free C-terminal segment is more likely to be the "reactive form" of ubiquitin rather than the N_1 itself. Although a detailed structure of N_2 must await further studies, the finding of two folded conformers in ubiquitin is expected to shed new light on the molecular mechanism of its biological function.

REFERENCES

1. Schneider, D. M., Dellwo, M. J., and Wand, A. J. (1992) *Biochemistry 31*, 3645−3652.
2. Lienin, S. F., Bremi, T., Brutscher, B., Brüschweiler, R., and Ernst, R. R. (1998) *J. Am. Chem. Soc. 120*, 9870−9879.
3. Cornilescu, G., Marquardt, J. L., Ottiger, M., and Bax, A. (1998) *J. Am. Chem. Soc. 120*, 6836−6837.
4. Woodward, C., Simos, I., and Tüchsen, E. (1982) *Mol. Cell. Biochem. 48*, 135−160.
5. Li, R., and Woodward, C. (1999) *Protein Sci. 8*, 1571−1591.
6. Rumbley, J., Hoang, L., Mayne, L., and Englander, S. W. (2000) *Proc. Natl. Acad. Sci. U.S.A. 98*, 105−112.
7. Yamada, H., Nishikawa, K., Honda, M., Shimura, T., Tabayashi, K., and Akasaka, K. (2001) *Rev. Sci. Instrum. 72*, 1463−1471.
8. Schlesinger, M., and Hershko, A., Eds. (1988) *The Ubiquitin System*, Cold Spring Harbor Laboratory, Cold Spring Harbor, NY.
9. Arrigo, A.-P., Tanaka., K., Goldberg, A. L., and Welch, W. J. (1988) *Nature 331*, 192−194.
10. Vijay-Kumar, S., Bugg, C. E., and Cook, W. J. (1987) *J. Mol. Biol. 194*, 531−544.
11. Di Stefano, D. L., and Wand, A. J. (1987) *Biochemistry 26*, 7272−7281.
12. Weber, P. L., Brown, S. C., and Mueller, L. (1987) *Biochemistry 26*, 7282−7290.
13. Pan, Y., and Briggs, M. S. (1992) *Biochemistry 31*, 11405−11412.
14. Li, H., Yamada, H., and Akasaka, K. (1999) *Biophys. J. 77*, 2801−2812.
15. Akasaka, K., Li, H., Yamada, H., Li, R., Thoresen, T., and Woodward, C. K. (1999) *Protein Sci. 8*, 1946−1953.
16. Inoue, K., Yamada, H., Akasaka, K., Herrmann, C., Kremer, W., Maurer, T., Döker, R., and Kalbitzer, R. (2000) *Nat. Struct. Biol. 7*, 547−550.
17. Kitahara, R., Sareth, S., Yamada, H., Ohmae, E., Gekko, K., and Akasaka, K. (2000) *Biochemistry 39*, 12789−12795.
18. Kuwata, K., Li, H., Yamada, H., Batt, C. A., Goto, Y., and Akasaka, K. (2001) *J. Mol. Biol. 305*, 1073−1083.
19. Bodenhausen, G., and Ruben, D. J. (1980) *Chem. Phys. Lett. 69*, 185−189.
20. Sklenar, V., Piotto, M., Leppic, R., and Saudek, V. (1993) *J. Magn. Reson., Ser. A 102*, 241−245.
21. Kitamura, Y., and Itoh, T. (1987) *J. Solution Chem. 16*, 715−725.
22. Farrow, N. A., Muhandiram, R., Singer, A. U., Pascal, S. M., Kay, C. M., Gish, G., Shoelson, S. E., Pawson, T., Forman-Kay, J. D., and Kay, L. E. (1994) *Biochemistry 33*, 5984−6003.
23. Li, H., Yamada, H., and Akasaka, K. (1998) *Biochemistry 37*, 1167−1173.
24. Li, H., Yamada, H., Akasaka, K., and Gronenborn, A. M. (2000) *J. Biomol. NMR 18*, 207−216.
25. Kaplan, J. I., and Fraenkel, G. (1980) *NMR of Chemically Exchanging Systems*, Academic Press, London.
26. Lipari, G., and Szabo, A. (1982) *J. Am. Chem. Soc. 104*, 4546−4559.
27. Lipari, G., and Szabo, A. (1982) *J. Am. Chem. Soc. 104*, 4559−4570.
28. Wang, A. C., Grzesiek, S., Tschuclin, R., Lodi, P. J., and Bax, A. (1995) *J. Biol. NMR 5*, 376−382.
29. Jonas, J., and Jonas, A. (1994) *Annu. Rev. Biophys. Biomol. Struct. 23*, 287−318.
30. Schick, M. (1998) Ph.D. Thesis, Eidgenössische Technische Hochschule, Switzerland.
31. Wishert, D. S., Bigam, C. G., Holm, A., Hodges, R. S., and Sykes, R. D. (1995) *J. Biomol. NMR 5*, 67−81.
32. Le, H., and Oldfield, E. (1994) *J. Biomol. NMR 4*, 341−348.
33. Akasaka, K., and Li, H. (2001) *Biochemistry 40*, 8665−8671.
34. Nicholls, A., Sharp, K. A., and Honig, B. (1991) *Proteins 11*, 281−296.
35. Bundi, A., and Wüthrich, K. (1979) *Biopolymers 18*, 299−312.
36. Kamatari, Y. O., Yamada, H., Dobson, C. M., and Akasaka, K. (2001) *Eur. J. Biochem. 268*, 1782−1793.

BI010922U